*F. ŽIVIĆ, M. BABIĆ, S. MITROVIĆ, P. TODOROVIĆ*

RESEARCH

# Interpretation of the Friction Coefficient During Reciprocating Sliding of Ti6Al4V Alloy Against $Al_2O_3$

*Tribological behaviour of Ti6Al4V alloy, during linear reciprocating sliding against alumina, at nanotribometer (ball-on-flat type of contact) was investigated. Experiments were carried out for sliding in Ringer's solution, over a range of loads (100 - 1000 mN) and speeds (4 - 12 mm/s). Friction behaviour of the contact pairs was investigated by analysis of the dynamic friction coefficient plots and effective root mean square (rms) coefficient of friction, $COF_{rms}$. Presented mathematical envelopes of dynamic coefficient of friction curves and averaged envelope signals provided additional explanation of one calculated $COF_{rms}$ value. Envelopes of dynamic coefficient of friction enabled easier determination of different periods during sliding, which were further related to wear mechanisms.*

***Keywords:*** *Dynamic friction coefficient; Ti6Al4V; Alumina; Nanotribometer.*

## 1. INTRODUCTION

Tribological applications in many new fields of advanced materials applications, such as biomedical implants, impose growing challenges for engineering materials. Titanium and titanium alloys has broad applications in a field of medicine [1-5]. Ti alloys are applied when high strength and low density ($4.5g/cm^3$) are of primary importance [5]. They are particularly interesting for biomedical applications because of their excellent biocompatibility and high corrosion resistance [6-8]. Implants made of titanium alloys tend to develop structural and functional connection between the living bone and the implant surface (osseointegration). Despite their good mechanical and chemical properties the use of Ti alloys is somehow limited due to their poor wear resistance. Ti6Al4V alloy has low sliding wear resistance because of its low resistance to plastic shearing during contact [1-10].

Ceramics are regarded as favorable materials for joints or joint surface materials. Conventional ceramics such as alumina ($Al_2O_3$) have been evaluated due to their excellent properties of high strength, good biocompatibility and stability in physiological environments [3]. Alumina can be polished to a high surface finish and has excellent wear resistance, and is often used for wear surfaces in joint replacement prostheses. Alumina is widely used for many tribological purposes such as medical prostheses, cutting tools, guides, dies or seals [9].

Sliding wear behaviour of Ti6Al4V alloy has been a subject to a relatively small number of investigations. Budinski [11] realised extensive research on tribological properties of titanium alloys and reported that Ti6Al4V has poor abrasion resistance. Masmoudi et al. [4] studied the influence of environment on friction coefficient values of Ti6Al4V alloy. Molinari et al. [6] studied mechanisms responsible for the wear resistance under different load and sliding speed conditions in self-mated Ti6Al4V disk-on-disk sliding tests. Several studies have been conducted to characterize tribological behaviour of Ti6Al4V alloy against alumina under different sliding conditions [9, 12]. The frictional behavior of selected orthopaedic titanium alloys during reciprocating-sliding was studied by Long and Rack [8] and they found it to be a function of contact stress, sliding velocity, cyclic count and alloy phase structure. Dong and Bell [9] reported unexpectedly high wear rates for alumina sliding against Ti6Al4V (pin-on-disk tests). They observed increase of the wear rate of alumina balls with increase of load or sliding speed and then wear rate decrease, i.e. typical transition

*F. Živić, M. Babić, S. Mitrović, P. Todorović*
*Tribology Laboratory, Faculty of Mechanical Engineering, Kragujevac, Serbia*
*E-mail: zivic@kg.ac.rs*

characteristics. Tribochemical reactions between Ti6Al4V and alumina surfaces were found responsible for the observed high wear rate of alumina. Qu et al. [12] observed large frictional fluctuations during contact of titanium alloys sliding against ceramic counterfaces (alumina). They also suggested possible tribochemical reactions between alumina sliders and Ti alloy disks. Corrosion behaviour of heat-treated Ti6Al4V alloy has been studied by Chang and Yang [13]. Zitnansky and Caplovic [14] and Ding et al. [26] showed that the structure of Ti6Al4V alloy can be greatly influenced by combined mechanical and thermal treatment. Dong and Bell reported enhanced wear resistance of titanium surfaces due to thermal oxidation treatment [16]. Fujii observed significant improvement of mechanical properties of Ti alloys by a series of heat treatment, solution treatment and aging [17]. However, the acting friction and wear mechanisms during sliding wear of titanium alloys have not been sufficiently addressed and understood and needs to be further studied [6-9, 16]. Investigations of friction and wear behavior on microscale level can further contribute to understanding of phenomena occurring during sliding of Ti6Al4V alloy.

Within this study, investigation of Ti6Al4V alloy during reciprocating sliding against alumina has been realised, by varying normal load and sliding speed. Alumina has significantly higher hardness than the titanium alloy, and shows outstanding abrasion resistance. Therefore, deformation processes during sliding can be assigned to Ti alloy only [12]. The aim of this study was to investigate possibilities of different interpretation of dynamic friction coefficient curves obtained by the tribometer and its relation to wear mechanisms during sliding.

## 2. MATERIALS AND EXPERIMENTAL METHODS

### 2.1 Materials

Ti6Al4V alloy was studied with chemical composition in mass percent of alloying elements: 6.1% Al, 3.95% V, 0.15% Fe, 0.14% O. Samples were cut (6.35 x 15.75 x 10.16 mm), from industrially produced bars, grounded with SiC paper and polished using 3 μm diamond suspension. Afterwards, Ti6Al4V alloy samples were annealed for 1 h at 750 $^{o}$C in Ar atmosphere. After annealing, the samples were cooled down to the room temperature in the furnace. Samples were then grounded with SiC paper (1000 grit). Final roughness of Ra=0.07μm were obtained by polishing samples with diamond paste on abrading wheel, thus obtaining initial roughness of Ra=0.3μm. Commercial alumina ($Al_2O_3$) ball of 1.5 mm diameter was used as the other material in contact.

### 2.2 Tribological tests

Sliding tests were carried out on a ball-on-flat configuration using CSM Nanotribometer Instrument. The scheme of the contact pair geometry is shown in Figure 1. Characteristics of conducted tribological tests are given in Table 1.

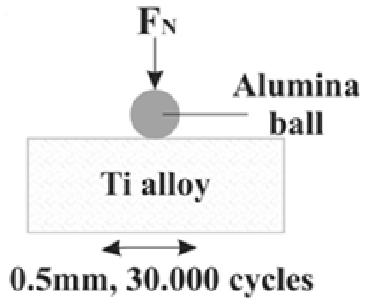


**Figure 1.** The scheme of the contact pair geometry

Ringer's solution, as laboratory solutions of salts in water, was used for lubrication, as simulated body fluids. It contains sodium chloride, potassium chloride, calcium chloride, and sodium bicarbonate in the concentrations in which they occur in body fluids. Composition of the Ringer's solution was (g per 1 liter of water): NaCl - 8.6; KCl - 0.30; CaCl2 - 0.33; Na+ 147.00 mmol; K+ 4.00 mmol; Ca+ 2.25 mmol; Cl+ 155.60 mmol. Ringer's solution was applied by immersing articulating surfaces totally in a solution.

Samples were prepared for testing in accordance with ASTM F136 - 02, ASTM F86 - 01, ASTM E1078 - 02. Each specimen was thoroughly cleaned by ethyl alcohol, then cleaned in ultrasonic bath for 60 minutes and dried in hot air afterwards. After that, samples were cleaned in isopropyl alcohol, by staying in the solution for 60 minutes and dried in a hot air. Samples were stored in a desiccator, prior to testing.

Duration of each test was 30000 cycles (distance of 30 m), whereat one cycle is represented by full amplitude sliding distance (half amplitude, 0.25mm). Selected sliding velocities lies in the range typically found in hip joints (0–50 mm/s) [18]. The friction coefficient, i.e. dynamic friction coefficient, was automatically recorded during the testing, using data acquisition software. Simultaneously, the friction coefficient curve was recorded and plotted.

**Table 1.** Tribological parameters

| **Instrument preferences** |
|---|
| Linear reciprocating module (linear mode acquisition)<br>Cantilever ST-111<br>$F_n$ stiffness: 1.7339 mN/μm with force range: 0.529 - 1733.9 mN;<br>$F_t$ stiffness: 4.2963 mN/μm with force range: 1.311 - 4296.3 mN)<br>Stroke: 0.5 mm<br>Ambient air temperature: approximately 25 °C<br>Sampling rate: 100 Hz |
| **Normal force values**, $F_n$: 100 mN, 250 mN, 500 mN, 750 mN, 1000 mN |
| **Maximum linear speed values**, $v$: 4 mm/s; 8 mm/s; 12 mm/s |

## 3. RESULTS AND DISCUSSION

### 3.1 Coefficient of friction

Diagrams of dynamic friction coefficient (COF) for selected regimes, during reciprocating sliding of Ti6Al4V alloy against $Al_2O_3$, as obtained by nanotribometer, are shown in Figure 2.

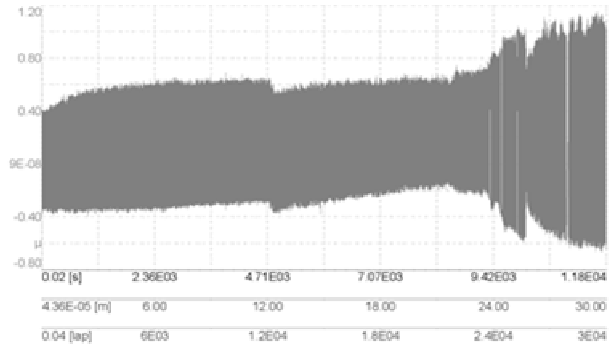

a)

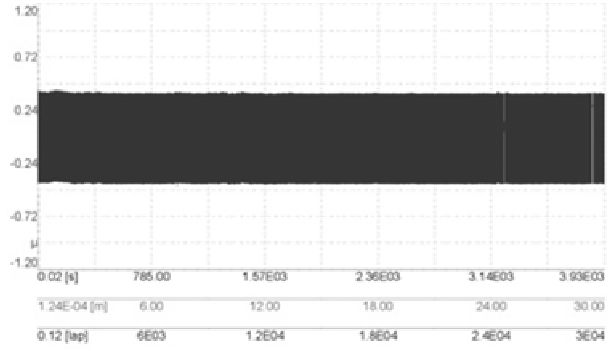

b)

**Figure 2.** Sample 3: Diagrams of dynamic friction coefficient, sliding in Ringer's solution: a) v=4 mm/s, $F_N$=100 mN; b) v=12 mm/s, $F_N$=1000 mN

The values of the friction coefficient were ranging from 0.4 to 1.2 and these values are similar to the results of previous studies [12]. Generally, increase of load produced lowering of the COF values. This decrease was especially prominent for higher values of sliding speed. In case of higher speed and higher loads regimes, steady-state value of the friction coefficient was reached shortly after the beginning of the test (approximately from 500 to 5000 cycles for all test conditions), as in Figure 2b. If regimes of lower speed and lower loads are observed, several zones can be distinguished on the friction coefficient curve (Figure 2b). At the beginning, values are lower increasing for one period of time, followed by a period of rather constant values. Then, at some point, sharp transition to higher COF values occurred, as in Figure 3a.

Considering high temperatures generated at the asperity contact between Ti6Al4V alloy and alumina, it is likely that the observed extremely high dynamic friction coefficient can be attributed to the tribochemical reactions occurring in the contact zone. It has been known that titanium is extremely active and ready to alloy with other materials, alumina as well [9]. Locally high temperatures at asperity contacts favor processes of adhesion and friction welding within a contact zone. Therefore, significantly higher force is needed to break bonds generated during contact and continue the sliding. This could be explanation for high COF values recorded during reciprocating sliding tests.

### 3.2 Analysis of the friction coefficient values obtained by the nanotribometer

Values of dynamic friction coefficient obtained during the test can be observed from different aspects, such as: start period value, mean value for the whole test, mean value during steady state period, maximum values for the whole period, maximum recorded differences in obtained values, value of standard deviation or any of these for specific period during sliding. Each of these parameters shows some specific information about

frictional behavior of the contact pair. However, it is important to adopt one common evaluation parameter in relation to friction coefficient that would best describe the whole process, since dynamic friction coefficient is exhibiting dynamic trend, not only one average value as in case of static friction coefficient.

It is possible to introduce one numerical value for observed period in each obtained COF diagram: effective root mean square (*rms*) coefficient of friction, $COF_{rms}$, thus reducing complex function to a single value. It is a common practice to use different averaging and filtering methods associated with sinusoidal signal in order to obtain more practical representation [22]. One of the usual parameters for description of the periodic function is root mean square of the function (abbreviated *rms*), also called "effective value" of the observed function. It is especially useful when variates are positive and negative, e.g., sinusoids. Rms is a statistical measure of the magnitude of a varying quantity. Since the obtained friction coefficient curve is of sinusoidal function type, it is possible to calculate *rms* value for each curve.

After each finished test, one .txt file was obtained as output file, with recorded COF values over time. Calculation of $COF_{rms}$ value, for each test, was done by applying the root mean square function to the raw data of friction coefficient recorded by the tribometer, according to the selected sampling rate frequency. $COF_{rms}$ values were calculated, for each test regime, using these data, according to the following equation:

$$\bar{X} = \sqrt{\frac{x_1^2 + x_2^2 + x_3^2 + ... + x_n^2}{n}}$$

where, $\bar{X}$ is $COF_{rms}$ value for one observed test, $x_i$ - numerical COF value recorded by nanotribometer device at *i* - point of time, *n* - number of recorded COF values by the tribometer during one test.

If calculated for the whole test duration for each performed test, $COF_{rms}$ values decreased with increase of normal load (Figure 2.). For higher loads, COF values were uniform over time (Figure 2b). If real time COF diagrams obtained from nanotribometer is considered (Figure 2a), it can be noticed that peaks distribution (maximum COF values) points to irregularities of different kind that influence frictional behavior. It can represent influence origination from surface roughness, accumulated wear debris, appearance of Ti oxides (e.g. $TiO_2$) in the contact zone or titanium-aluminium intermetallic compounds ($Ti_2Al_3$, $Al_3Ti$) produced during sliding of Ti alloy against $Al_2O_3$. Dong and Bell [9] proved that $Ti_2Al_3$ particles appear during sliding. Therefore, distribution and/or appearance of various isolated peaks that occur within these COF diagrams can be important indicator of different influences.

Peaks distribution along COF curve can be identified by applying mathematical envelope function on the unprocessed signal experimentally obtained from the tribometer. Mathematical envelope of COF curves shown in Figure 2. are shown in Figure 3.

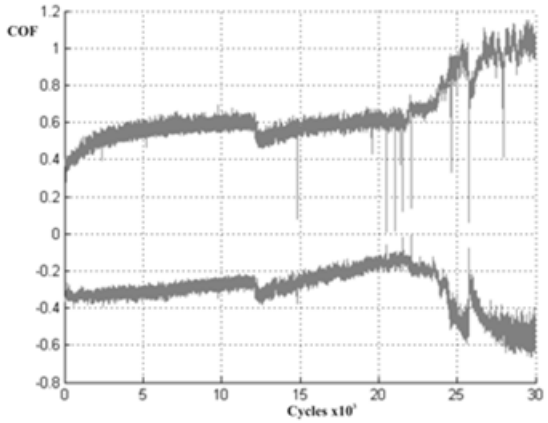


a)

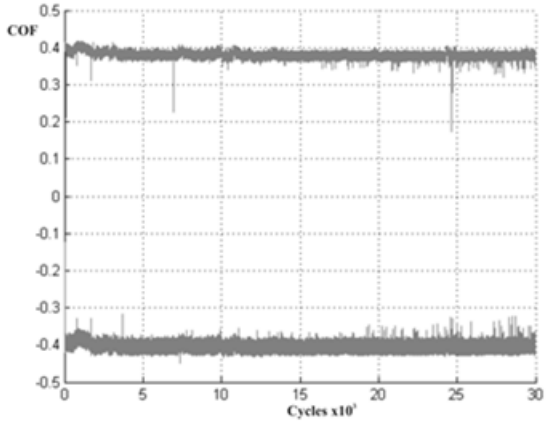


b)

**Figure 3.** Mathematical envelope of COF curve: v=4 mm/s; $F_N$=100mN; b) v=12 mm/s; $F_N$=1000mN;

Further filtration of the obtained envelope signal (Figure 3.) can be done by averaging it using simple moving average method. In this way, lowering of the noise level in the curve is achieved. Averaging of the signal is done separately for the upper and the lower parts of the previously obtained envelopes (Figure 3.), what is shown in Figure 4.

Averaged envelope signals presented in Figure 4. represent friction coefficient variation curve for linear reciprocating sliding of the flat sample-ball contact at CSM nanotribometer device. It can point to certain periods of the wear process during sliding. Periods of different wear mechanisms can also be identified based on COF behavior. Three different periods can be determined in Figure 4a.

The first period of sliding is characterized by constant significant increase of COF values, corresponding to initial period of the wear. The second period can be described as steady state friction even though some fluctuation of COF values occurred. The third period of sliding is characterized by sharp transition to extremely high COF values indicating some significant changes in the contact zone.

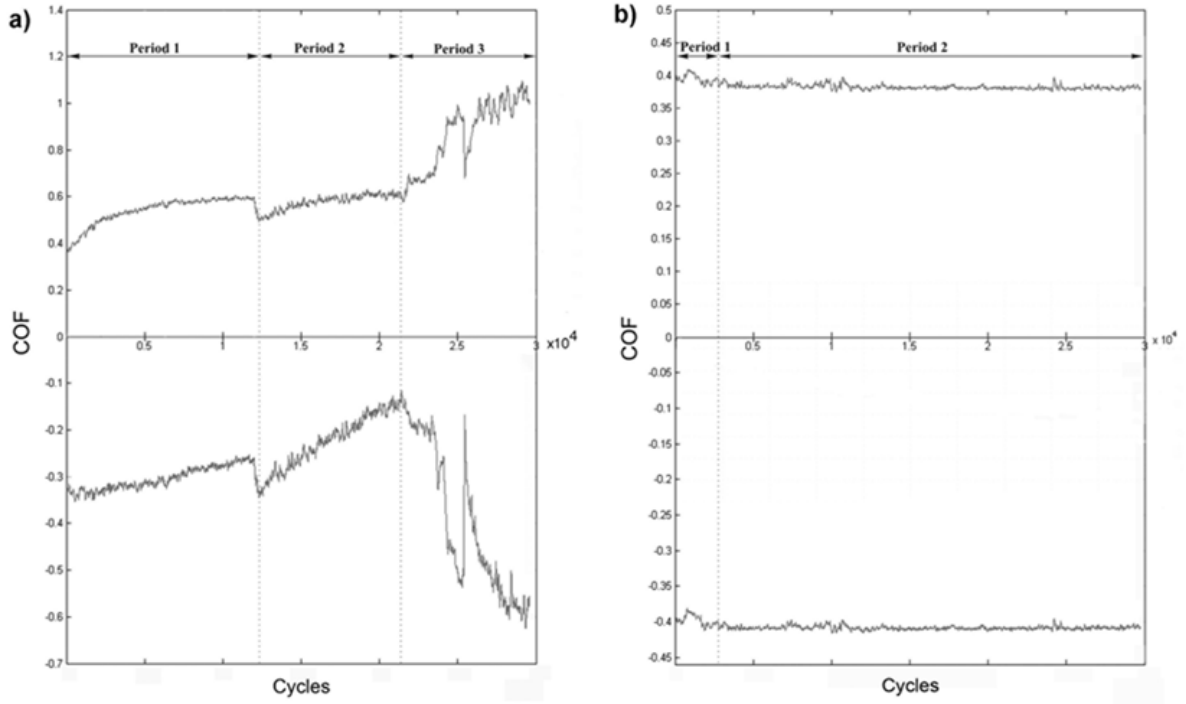


**Figure 4.** Averaging of the envelope signal of COF curve: a) v=4 mm/s; $F_N$=100mN; b) v=12 mm/s; $F_N$=1000mN

This behavior of friction coefficient curve is well related to literature [23, 6-9, 12], where authors proved that wear mechanisms change during the sliding of Ti6Al4V against $Al_2O_3$ and also change with load and speed variation.

As studied in the literature, the first period of sliding is governed by mixed adhesive and tribochemical wear leading to production of wear debris accompanied and supported by chemical reactions of Ti alloy with environment and $Al_2O_3$. When certain critical quantities of wear debris is generated, abrasive wear starts to appear together with adhesive wear (period 2 in Figure 4.) during which wear debris is periodically ejected away from the contact zone (oscillation of COF values). The third period is governed by the severe abrasive and delamination wear probably due to large quantities of wear debris influenced also by the hard $Ti_2Al_3$ particles as per literature [9].

In case of the other selected example in Figure 4b, there is rather uniform distribution of COF values, except for a slight change during the beginning period. As per literature [23, 6-9], high sliding velocity and high normal load influence quite different wear mechanisms if compared to low speed and load. This difference is clearly seen in Figure 4. In case of high speed and load (Figure 4b), friction is greatly influenced by frictional heating which produce softening of the Ti6Al4V alloy surface. This in return favors plastic flow and mild adhesive and abrasive wear with no evidence of larger quantities of wear debris [23]. Also, a stable oxide layer formed as a result of a high flash temperature [20], which provides separation of contact surfaces and wear decrease. There is no significant fluctuation of COF values and steady state period (period 2 in Figure 4b) is achieved shortly after the beginning of the test.

According to the previous, calculation of $COF_{rms}$ values for dynamic coefficient curve can be done for different periods of sliding for each test. It is important to notice that one $COF_{rms}$ value can be obtained for different shapes of COF curves [23]. Filtering of the signal can be done with different

degree of filtering. If high filtering is applied some specific events of frictional behavior cannot be observed and compared to wear behavior. On the other side, some moderate filtering of the signal can point out to the most significant moments of frictional behavior of the sample. Presented mathematical envelopes of COF curves (Figure 3.) and averaged envelope signals (Figure 4.) provide additional explanation of one calculated $COF_{rms}$ value. They enable efficient determination of different periods during sliding, in order to define which period to take into account. They also indicate changes of wear mechanisms during one test, if there are any observed.

## 4. CONCLUSIONS

Different approaches in interpretation of dynamic friction coefficient may provide dispersion of test results. Introduced effective root mean square (*rms*) coefficient of friction, $COF_{rms}$, represented plot of dynamic coefficient of friction by one numerical value. However, one single numerical value can represent different trends of dynamic friction coefficient. Presented mathematical envelopes of COF curves and averaged envelope signals provided additional explanation of one calculated $COF_{rms}$ value. Envelopes of dynamic coefficient of friction enabled easier determination of different periods during sliding, which were further related to wear mechanisms.

**Acknowledgement**

This study was financed by Ministry of Science and Technological Development, Serbia, project No.35021.

## REFERENCES

[1] Buckley, D.H.: *Friction differences between aliphatic and aromatic structures in lubrication of titanium*, NASA technical note, NASA TN D-8088, 1975

[2] Black, J., Hastings, G., (ed.), *Handbook of Biomaterial Properties*, Chapman & Hall, London, 1998

[3] Geetha, M., Singh, A.K., Asokamani, R., Gogia, A.K.: *Ti based biomaterials, the ultimate choice for orthopaedic implants – A review*, Progress in Materials Science 54, 397–425, 2009

[4] Masmoudi, M., Assoul, M., Wery, M., Abdelhedi, R., El Halouani, F., Monteil, G.: *Friction and wear behaviour of cp Ti and Ti6Al4V following nitric acid passivation*, Applied Surface Science 253, 2237–2243, 2006

[5] Enderle, J.D., Blanchard, S.M., Bronzino, J.D.: *Introduction to Biomedical Engineering*, Second Edition, Elsevier, Amsterdam, 2005

[6] Molinari, A., Straffelini, G., Tesi, B., Bacci, T.: *Dry sliding wear mechanism of the Ti6Al4V alloy*, Wear 208, 105-112, 1997

[7] Straffelini, G., Molinari, A.: *Dry sliding wear of Ti–6Al–4V alloy as influenced by the counterface and sliding conditions*, Wear 236, 328–338, 1999

[8] Long, M., Rack, H.J.: *Friction and surface behavior of selected titanium alloys during reciprocating-sliding motion*, Wear 249, 158–168, 2001

[9] Dong, H., Bell, T.: *Tribological behaviour of alumina sliding against Ti6Al4V in unlubricated contact*, Wear 874–884, 1999

[10] Walker, P.S., Blunn, G.W., Lilley, P.A.: Wear *Testing of Materials and Surfaces for Total Knee Replacement*, Journal of Biomedical Materials Research (Applied Biomaterials) 33, 159-175, 1996

[11] Budinski, K.G.: *Tribological properties of titanium alloys*, Wear 151, 203-217, 1991

[12] Qu, J. Blau, P.J., Watkins, T.R., Cavin, O.B., Kulkarni, N.S.: *Friction and wear of titanium alloys sliding against metal, polymer, and ceramic counterfaces*, Wear 258, 1348–1356, 2005

[13] Chang, T.M.L.E., Yang C.Y.: *A comparison of the corrosion behaviour and surface characteristics of vacuum-brazed and heat-treated Ti6Al4V alloy*, Journal of Materials Science: Materials in Medicine 9, 429-437, 1998

[14] Zitnansky, M., Caplovic L.: *Effect of the thermomechanical treatment on the structure of titanium alloy Ti6Al4V*, Journal of Materials Processing Technology 157–158, 643–649, 2004

[15] Ding, R., Guo, Z.X., Wilson A.: *Microstructural evolution of a Ti–6Al–4V alloy during thermomechanical processing*, Materials Science and Engineering A327, 233–245, 2002

[16] Dong, H., Bell, T.: *Enhanced wear resistance of titanium surfaces by a new thermal oxidation treatment*, Wear 238, 131–137, 2000

[17] Fujii, H.: *Strengthening of α+β titanium alloys by thermomechanical processing*, Materials Science and Engineering A243, 103–108, 1998

[18] Gispert, M.P., Serro, A.P., Colaco, R., Saramango B.: *Friction and wear mechanisms in hip prosthesis: Comparison of joint materials behaviour in several lubricants*, Wear 260, 149-158, 2006

[19] Hager, C.H Jr., Sanders, J.H., Sharma, S.: *Effect of high temperature on the characterization of fretting wear regimes at Ti6Al4V interfaces*, Wear 260, 493-508 (2006)

[20] Lee, W.S, Lin, C.F.: *High-temperature deformation behaviour of Ti6Al4V alloy evaluated by high strain-rate compression tests*, Journal of Materials Processing Technology 75, 127–136 (1998)

[21] Vairis, A., Frost, M.: *Modelling the linear friction welding of titanium blocks*, Materials Science and Engineering A, 292, 8-17, 2000

[22] L. Nechak, S. Berger, E. Aubry, *A polynomial chaos approach to the robust analysis of the dynamic behaviour of friction systems*, European Journal of Mechanics - A/Solids, 2011

[23] F. Zivic, M. Babic, S.Mitrovic, A. Vencl, *Continuous control as alternative route for wear monitoring by measuring penetration depth during linear reciprocating sliding of Ti6Al4V alloy*, Journal of Alloys and Compounds, Vol. 509, 5748-5754, 2011